Solution of the multistep pathway for assembly of corynanthean, strychnos, iboga, and aspidosperma monoterpenoid indole alkaloids from 19*E*-geissoschizine

Yang Qu[a], Michael E. A. M. Easson[a,1], Razvan Simionescu[b], Josef Hajicek[b,2], Antje M. K. Thamm[a,3], Vonny Salim[a,4], and Vincenzo De Luca[a,5]

[a]Department of Biological Sciences, Brock University, St. Catharines, ON L2S 3A1, Canada; and [b]Department of Chemistry, Brock University, St. Catharines, ON L2S 3A1, Canada

Edited by Jerrold Meinwald, Cornell University, Ithaca, NY, and approved February 11, 2018 (received for review November 16, 2017)

Monoterpenoid indole alkaloids (MIAs) possess a diversity of alkaloid skeletons whose biosynthesis is poorly understood. A bioinformatic search of candidate genes, combined with their virus-induced gene silencing, targeted MIA profiling and in vitro/in vivo pathway reconstitution identified and functionally characterized six genes as well as a seventh enzyme reaction required for the conversion of 19*E*-geissoschizine to tabersonine and catharanthine. The involvement of pathway intermediates in the formation of four MIA skeletons is described, and the role of stemmadenine-*O*-acetylation in providing necessary reactive substrates for the formation of iboga and aspidosperma MIAs is described. The results enable the assembly of complex dimeric MIAs used in cancer chemotherapy and open the way to production of many other biologically active MIAs that are not easily available from nature.

Catharanthus roseus monoterpeoind indole alkaloids | virus-induced gene silencing | catharanthine assembly | tabersonine assembly | multiple-pathway gene function

Monoterpenoid indole alkaloids (MIAs), with several thousand reported chemical structures, are one of the most diverse classes of plant specialized metabolites (1–3). Known to harbor various biological activities, numerous MIAs provide a rich source of medicinal products. Examples include the anticancer compounds vinblastine and vincristine from *Catharanthus roseus* (Madagascar periwinkle) and camptothecin from *Camptotheca acuminata*. The scarcity of these MIAs in nature combined with their complex structures that challenge chemical synthesis, have often impeded proper evaluation of their medicinal value. Recently, the rare nor-stemmadenine type MIA, conolidine, originally identified in the heartwood of *Tabernaemontana divaricata*, was synthesized and found to have potent analgesic activity, making it a promising nonopioid alternative in combatting persistent pain (4).

Almost all MIAs are derived from the central intermediate, strictosidine that upon β- glucosidase hydrolysis affords highly malleable aglycone intermediates that are converted to numerous MIA backbones (1, 3). Lately, the entire iridoid pathway leading to the formation of strictosidine was elucidated, providing the foundation for assembly of thousands of MIAs in microorganisms (5–10). Vindoline, one of the two structural monomers that combines with catharanthine to generate the anticancer drug 3,4-anhydrovinblastine and synthetic derivatives, was also produced in yeast via a seven-step pathway from the MIA precursor tabersonine (11). However, the multistep pathways linking strictosidine to the formation of the iboga MIA, catharanthine and the aspidosperma MIA, tabersonine remain poorly understood. The discovery of the genes involved and their functional characterization provides keys to the formation of these backbones and to the biotechnological production of a broad range of MIAs of potential medicinal value, in addition to catharanthine and tabersonine.

This report describes the discovery and functional characterization of six genes as well as a seventh enzyme reaction required for the formation of tabersonine or catharanthine from 19*E*-geissoschizine. Gene discovery involved a combination of bioinformatics and virus-induced gene silencing (VIGS) to identify candidate genes and functional expression of the selected genes by in vitro/in vivo reconstitution of the pathway. A series of highly unstable intermediates that rearrange to other important MIA precursors when not used by appropriate enzymes reveals the plasticity of MIA formation and how this fundamental property led to diverse MIA structures found in nature.

Results

VIGS Identifies Candidate Genes for the Conversion of 19*E*-Geissoschizine to Stemmadenine in the Pathway to Iboga/Aspidosperma MIAs. The assembly of MIAs in the leaf epidermis of *C. roseus* is associated with the secretion of catharanthine to the leaf surface and the transport of desacetoxyvindoline to

Significance

The multistep assembly of catharanthine and tabersonine from strictosidine remains poorly characterized for understanding the biochemistry of anticancer monoterpenoid indole alkaloid (MIA) biosynthesis in the medicinal plant, *Catharanthus roseus*. The seven-step pathway from 19*E*-geissoschizine to four major MIA skeletons enables the assembly of catharanthine and tabersonine that complete the pathway for biosynthesis of the anticancer drugs, anhydrovinblastine and vincristine as well as for production of other biologically active MIAs.

Author contributions: Y.Q., A.M.K.T., V.S., and V.D.L. designed research; Y.Q., A.M.K.T., and V.S. performed research; Y.Q., M.E.A.M.E., and R.S. contributed new reagents/analytic tools; Y.Q., M.E.A.M.E., R.S., J.H., and V.D.L. analyzed data; and Y.Q., J.H., and V.D.L. wrote the paper.

Conflict of interest statement: V.D.L. and Y.Q. have filed a patent (PCT/CA2017/050284).

This article is a PNAS Direct Submission.

Data deposition: The sequences reported in this paper have been deposited in the GenBank database [accession nos. geissoschizine synthase (MF770507), geissoschizine oxidase (MF770508), Redox1 (MF770509), Redox2 (MF770510), stemmadenine-*O*-acetyltransferase (MF770511), hydrolase1 (MF770512), hydrolase2 (MF770513), hydrolase3 (MF770514), and hydrolase4 (MF770515)].

[1]Present address: Department of Biochemistry, Max Planck Institute for Chemical Ecology, D-07745 Jena, Germany.

[2]Present address: Department of Organic Chemistry, Faculty of Science, Charles University in Prague, 128 43 Prague 2, Czech Republic.

[3]Present address: Havas Life Bird & Schulte, 79102 Freiburg, Germany.

[4]Present address: Department of Biochemistry and Molecular Biology, Michigan State University, East Lansing, MI 48824.

[5]To whom correspondence should be addressed. Email: vdeluca@brocku.ca.

This article contains supporting information online at www.pnas.org/lookup/suppl/doi:10.1073/pnas.1719979115/-/DCSupplemental.

Published online March 6, 2018.

specialized leaf mesophyll cells for a two-step conversion to vindoline (12–14). Therefore, an expressed sequence tag (EST) dataset highly enriched in *C. roseus* leaf epidermal transcripts, previously used in the discovery of MIA pathway genes (11, 12, 14), was investigated. We hypothesize that (*i*) catharanthine/tabersonine biosynthetic genes should be well represented in this dataset, (*ii*) the pathway is conserved in other Apocynaceae plants that also make iboga/aspidosperma type MIAs, and (*iii*) the pathway is not conserved in non-MIA producing species. A short list of transcripts with EST counts greater than five that encode proteins less than 70% identical to *Arabidopsis* homologs and that are conserved in *Vinca minor, Amsonia hubrichtii*, and *Tabernaemontana elegans* (alignment *E* value $<10^{170}$) were selected. The resulting short list of 65 genes (Dataset S1) contained 4 known MIA pathway genes (loganic acid methyltransferase, secologanin synthase, tryptophan decarboxylase, and strictosidine synthase), as well as 13 candidate genes that were selected for VIGS studies. Targets included likely cytochrome P450s, oxidoreductases, and hydrolases involved in MIA biosynthesis.

The performance of VIGS combined with LC-MS analyses of MIA profiles yielded plants with altered profiles for five candidate genes compared with controls (Fig. 1) that were selected for further biochemical and molecular characterization. This strategy together with the recent discovery of a high ajmalicine

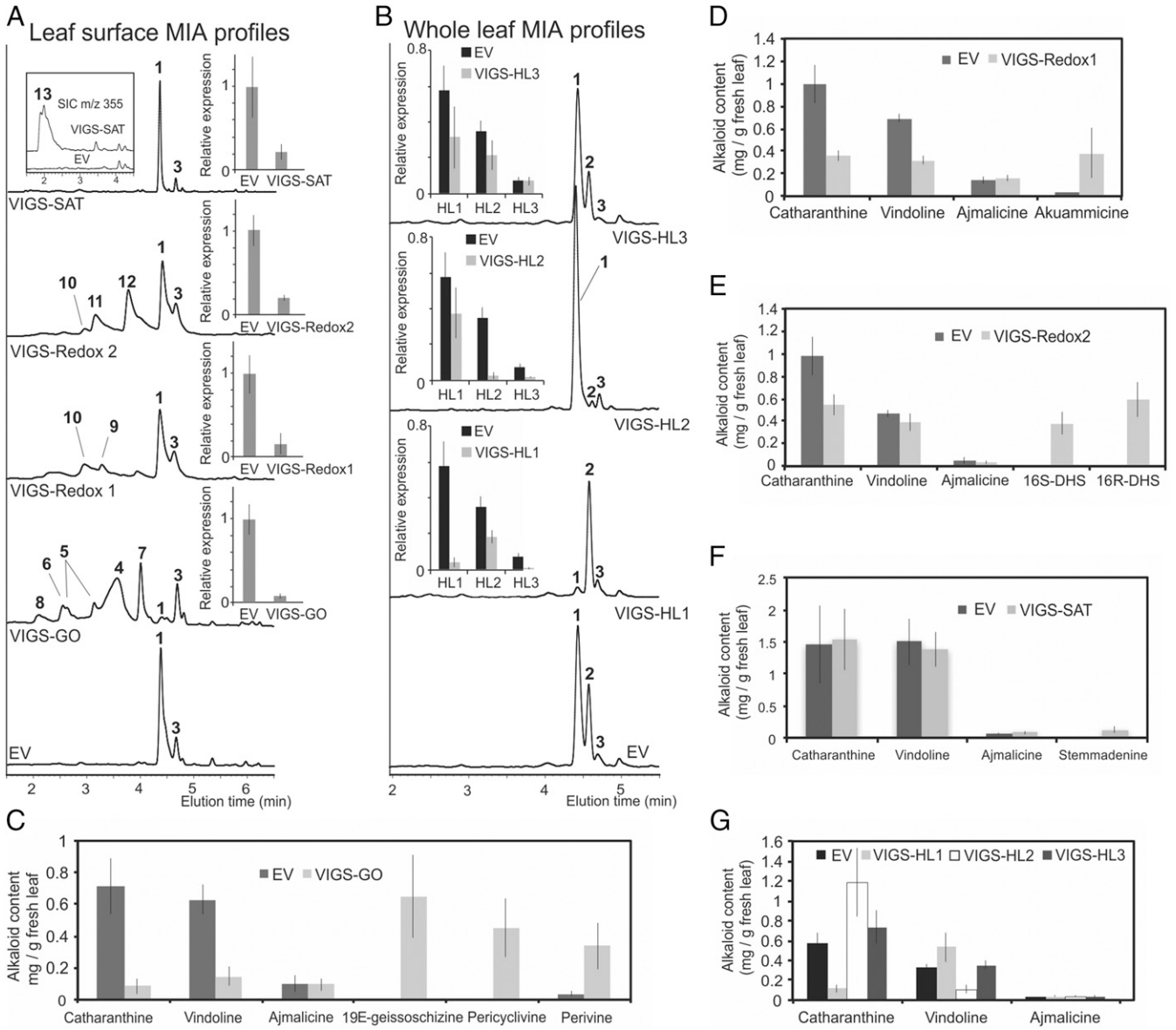

Fig. 1. VIGS silencing of GO, Redox1, Redox2, SAT, HL1, HL2, and HL3 results in accumulation of intermediates that reveal their involvement in the assembly of catharanthine and tabersonine. (*A*) Representative LC-chromatograms (280 nm) of leaf surface MIAs extracted in chloroform and mean relative expression levels by qRT-PCR of respective genes of VIGS plants silenced for geissoschizine oxidase (GO), Redox1, Redox2, and stemmadenine-*O*-acetyltransferase (SAT), compared with empty vector (EV) controls. (*B*) Representative LC-chromatograms (280 nm) of whole leaf MIAs extracted in ethyl acetate and mean relative expression levels by qRT-PCR of respective genes of VIGS plants silenced for Hydrolases 1–3 (HL1–HL3) compared with EV controls. (*C*–*G*) MIA contents in leaves of VIGS–GO, –Redox1, –Redox2, –SAT, and –HL1, -2, and -3 compared with the EV controls. Biological replicates = 5. Error bars represent the SD. Peak identification: **1**, catharanthine; **2**, vindoline; **3**, ajmalicine; **4**, 19*E*-geissoschizine; **5**, 19*E*-geissoschizine methanol adducts that disappear when dissolved in acetonitrile; **6**, 16*R*,19*E*-isositsirikine; **7**, pericyclivine; **8**, perivine; **9**, short-lived MIA of *m/z* 369; **10**, akuammicine; **11**, 16*S*-deshydroxymethylstemmadenine (DHS); **12**, 16*R*-DHS; and **13**, stemmadenine that shows structural fluctuation (splitting peaks) when analyzed by LC-MS. See Fig. 3 for respective structures.

accumulating *C. roseus* mutant led to the discovery of a cinnamyl alcohol dehydrogenase-type gene, geissoschizine synthase (GS) (15), the gateway step in iboga and aspidosperma MIA biosynthesis. Expression and biochemical characterization of geissoschizine synthase in *Escherichia coli* was important for the enzymatic production of 19*E*- and 19*Z*-geissoschizine (15) since in another study enzyme assays with recombinant protein from *E. coli* expressing the same gene (16) generated the 19-epimers of 16*R*-isositsirikine rather than 19*E*- and 19*Z*-geissoschizine.

The first VIGS candidate was a cytochrome P450 gene previously reported as CYP71AY2 (9) or CYP71D1v1 (17) with no known function. VIGS suppressed these transcripts by 92.2% and decreased both catharanthine and vindoline levels by 88.2% (Fig. 1 *A* and *C* and *SI Appendix*, Fig. S1*A*) and 77.0% (Fig. 1*C* and *SI Appendix*, Fig. S1*B*), respectively, compared with the empty vector (EV) control. The decline of catharanthine/vindoline was replaced by increases of 19*E*-geissoschizine (Fig. 1*A*, peak 4, Fig. 1*C*, and *SI Appendix*, Fig. S1*A*) and adducts (Fig. 1*A*, peak 5, Fig. 1*C*, and *SI Appendix*, Fig. S1*A*), 16*R*, 19*E*-isositsirikine (Fig. 1*A*, peak 6 and *SI Appendix*, Fig. S1*A*), pericyclivine (Fig. 1*A*, peak 7, Fig. 1*C*, and *SI Appendix*, Fig. S1*A*), and perivine (Fig. 1*A*, peak 8, Fig. 1*C*, and *SI Appendix*, Fig. S1*A*) in the VIGS line compared with the EV control lines (Fig. 1 *A* and *C* and *SI Appendix*, Fig. S1 *A* and *B*). The VIGS results suggest that this gene may encode geissoschizine oxidase (GO). The identity of perivine was confirmed by comparing it to authentic standard, while those of 19*E*-geissoschizine, pericyclivine, and 16*R*, 19*E*-isositsirikine were resolved by NMR analyses (*SI Appendix*, Figs. S2–S8 and Tables S1 and S2). The detection of the sarpagan MIAs, pericyclivine and perivine, in VIGS-GO plants suggest that their biosynthesis branches off from iboga and aspidosperma MIAs after the formation of strictosidine aglycones or 19*E*-geissoschizine. A separate VIGS-GO study (16) showed that silenced plants accumulated 16*R*, 19*E*-isositsirikine in lines with reduced catharanthine/vindoline, but not the other MIAs described in the present study.

The second gene submitted to VIGS was a cinnamyl alcohol dehydrogenase-like enzyme (54% amino acid identity to GS) named Redox1. VIGS suppressed Redox1 by 85.2% and reduced catharanthine and vindoline levels by 64.1% (Fig. 1 *A* and *D* and *SI Appendix*, Fig. S1*C*) and 53.8% (Fig. 1*D* and *SI Appendix*, Fig. S1*D*), respectively, compared with the EV controls. The decline of catharanthine/vindoline was replaced by increases of akuammicine (Fig. 1*A*, peak 10; Fig. 1*D*; and *SI Appendix*, Fig. S1*C*) and a short-lived MIA (*m/z* 369) (Fig. 1*A*, peak 9, Fig. 1*D*, and *SI Appendix*, Fig. S1*C*). Identification of akuammicine was confirmed by NMR analysis after purification of this MIA by preparative TLC (*SI Appendix*, Figs. S9 and S10 and Tables S1 and S2). Interestingly, the short-lived MIA (*m/z* 369) was spontaneously converted to akuammicine within 1 h (*SI Appendix*, Fig. S11), therefore preventing further NMR analysis.

The third gene submitted to VIGS was an aldo-keto–type reductase named Redox2. VIGS suppressed Redox2 by 79.4% and reduced catharanthine and vindoline levels by 44.2% (Fig. 1 *A* and *E* and *SI Appendix*, Fig. S1*E*) and 15.8% (Fig. 1*E* and *SI Appendix*, Fig. S1*F*), respectively, compared with the EV controls. The decline of catharanthine and vindoline was replaced by increases of 16*S*- (Fig. 1*A*, peak 11, Fig. 1*E*, and *SI Appendix*, Fig. S1*E*) and 16*R*-deshydroxymethylstemmadenine (DHS) (Fig. 1*A*, peak 12, Fig. 1*E*, and *SI Appendix*, Fig. S1*E*) epimers in the suppressed line. The identity of 16*S*- and 16*R*-DHS was confirmed by NMR analyses of MIAs purified by preparative TLC (*SI Appendix*, Figs. S12–S16 and Tables S1 and S2).

Enzymatic Conversion of 19*E*-Geissoschizine to Stemmadenine Involves Concerted Reactions of Geissoschizine Oxidase, Redox1 and Redox2. A GO-yeast strain was used to isolate yeast microsomes containing recombinant protein. Enzyme assays with GO microsomes

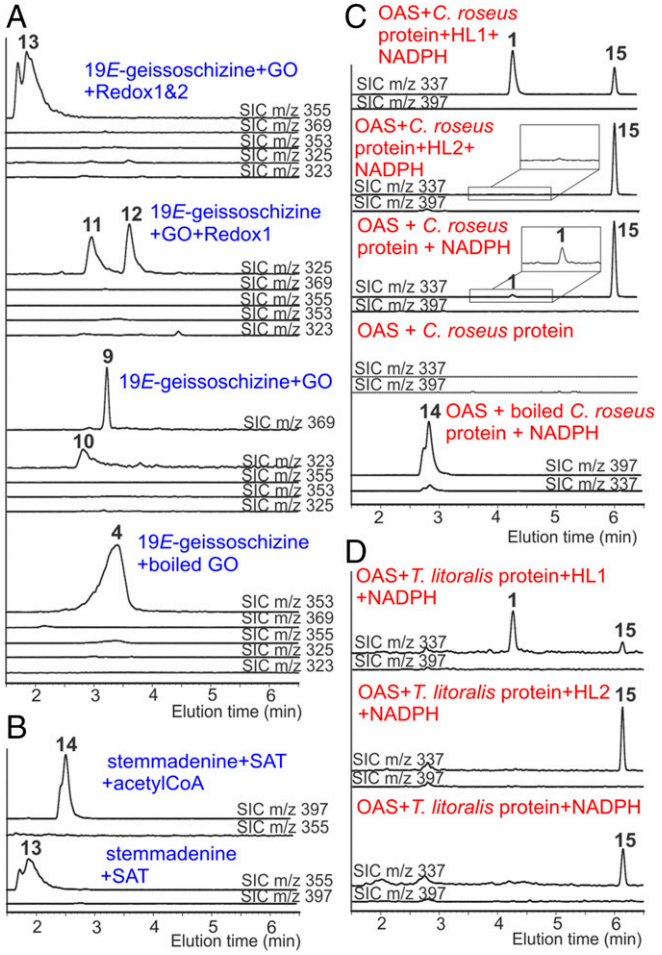

Fig. 2. Functional expression and establishment of biochemical function of GO, Redox1, Redox2, SAT, HL1, and HL2. (*A*) MIA formation when using 19*E*-geissoschizine and various combinations of yeast microsomes containing GO and recombinant enzymes purified from *E. coli*. (*B*) Conversion of stemmadenine to *O*-acetylstemmadenine (OAS) using recombinant SAT purified from *E. coli*. (*C*) Formation of catharanthine or tabersonine using OAS, crude leaf proteins of *C. roseus*, and recombinant HL1/HL2 purified from *E. coli*. (*D*) Formation of catharanthine or tabersonine using OAS, crude leaf proteins of *T. litoralis*, and recombinant HL1/HL2 purified from *E. coli*. Each trace shows the selected ion chromatogram (SIC). Peak identification: **14**, *O*-acetylstemmadenine that shows structural fluctuation (splitting peaks) when analyzed by LC-MS and **15**, tabersonine. See Fig. 3 for respective structures.

and NADPH converted 19*E*-geissoschizine (*m/z* 353) to akuammicine (Fig. 2*A*, peak 10; *m/z* 323; max 229, 292, and 328 nm) and the same short-lived MIA (*m/z* 369; max 227 and 279 nm; Fig. 2*A*, peak 9) that were both detected in VIGS–Redox1 plants (Fig. 1*A*, peaks 9 and 10). The mass increase of 16 from 19*E*-geissoschizine (*m/z* 353) suggested that the short-lived MIA (*m/z* 369) might be an oxidation product of 19*E*-geissoschizine. Together the VIGS data (Fig. 1 *A* and *C*) and the GO enzyme assays (Fig. 2*A*) confirmed this enzyme was geissoschizine oxidase. The loss of C(17) to form akuammicine makes it an unlikely intermediate in the assembly of catharanthine or tabersonine that would retain C(17). This was confirmed by the failure of affinity-purified recombinant Redox1 to convert akuammicine or the short-lived MIA to any new products, while the coupled reaction with GO and Redox1 converted 19*E*-geissoschizine to 16*S* (Fig. 2*A*, peak 11) and 16*R* (Fig. 2*A*, peak 12) epimers of DHS that were also observed in VIGS–Redox2 plants (Fig. 1*A*, peaks 11 and 12). Since both epimers of DHS are also missing C(17) they also may be breakdown

products of a highly unstable intermediate actually involved in catharanthine/tabersonine biosynthesis.

While Redox2 was unable to convert the 16*S* and 16*R* epimers of DHS to any other MIAs, it did catalyze the stereospecific reduction (18) of 19*E*-/19*Z*-geissoschizine to 16*R*-isositsirikine (*SI Appendix*, Fig. S17), therefore explaining the accumulation of 16*R*, 19*E*-isositsirikine (Fig. 1*A*, peak 6) when 19*E*-geissoschizine accumulated in VIGS–GO plants. Reduction of 19*E*-/19*Z*-geissoschizine with $NaBH_4$ yielded both 16*R*- and 16*S*-isositsirikine (*SI Appendix*, Fig. S17) and their identity was verified by NMR analyses (*SI Appendix*, Figs. S7, S8, and S18–S20 and Tables S1 and S2). While isositsirikine or DHS were not substrates for GO and/or Redox1, when all three recombinant proteins were incubated in the presence of NADPH, 19*E*-geissoschizine was converted to a new MIA (*m*/*z* 355) (Fig. 2*A*, peak 13). Similarly, yeast coexpressing GO, Redox1, and Redox2 converted 19*E*-geissoschizine to larger amounts of this MIA (*SI Appendix*, Fig. S21) that was purified by preparative TLC. NMR analyses identified it as stemmadenine (*SI Appendix*, Figs. S22–S24 and Tables S1 and S2), a proposed critical intermediate (19, 20) in the tabersonine/catharanthine pathway.

VIGS Identifies Two Candidate Genes Involved in the Catharanthine and Tabersonine Branch Pathways, Respectively. The last two candidate genes submitted to VIGS belong to a small family of four homologous (78–83% amino acid identity) α/β hydrolases (named HL1–HL4 based on descending EST counts, Dataset S1). The low EST counts for HL4 eliminated it from further analysis, while quantitative-PCR analyses suggested that HL1 (58.0% abundance) and HL2 (35.0% abundance) composed the major HL transcripts in *C. roseus* leaves compared with HL3 (7.0% abundance). Regions with least amino acid sequence similarity (*SI Appendix*, Fig. S25) were selected for design of VIGS–HL1, -2, and -3 vectors. When HL1 transcripts were reduced by 92.4% compared with EV controls, those of HL2 and HL3 also declined by 52.9% and 90%, respectively (Fig. 1*B*). When HL2 transcripts were reduced by 92% those of HL1 and HL3 also declined by 35.2% and 74.3%, respectively (Fig. 1*B*). Silencing of HL3 by VIGS–HL3 failed to alter HL3 transcript levels while those of HL1 and HL2 declined by 45.9% and 38%, respectively (Fig. 1*B*). When HL1 was the silencing target, catharanthine levels declined by 80.1% (Fig. 1*B*, peak 1 and Fig. 1*G*) and vindoline levels increased to 164% (Fig. 1*B*, peak 2 and Fig. 1*G*), while silencing of HL2 decreased vindoline levels by 65.5% (Fig. 1*B*, peak 2 and Fig. 1*G*) and increased catharanthine levels to 210% (Fig. 1*B*, peak 1 and Fig. 1*G*). When HL3 was the silencing target, no significant MIA changes were detected (Fig. 1 *B* and *G*) and no other MIA changes were detected in any of the HL-silenced plants. The altered MIA phenotypes generated by silencing HL1 and HL2 suggested that HL1 and HL2 rather than HL3 catalyze biochemical reactions in the catharanthine and tabersonine branch pathways, respectively.

Stemmadenine-*O*-Acetylation Is Required for the Biosynthesis of Catharanthine and Tabersonine. When yeast coexpressing GO, Redox1, Redox2, HL1, and HL2 were provided with 19*E*-geissoschizine they accumulated stemmadenine but no additional MIAs. Similarly, cell-free assays containing 19*E*-geissoschizine, NADPH, and the five recombinant proteins generated only stemmadenine. The results suggested that additional enzymes were required to convert stemmadenine to an MIA substrate that could be used by HL1 in the formation of catharanthine and by HL2 in the formation of tabersonine.

To identify the missing steps, 19*E*-geissoschizine and NADPH were incubated with the five recombinant enzymes and crude *C. roseus* leaf proteins. The addition of acetyl CoA to the enzyme mixture converted 19*E*-geissoschizine to catharanthine and tabersonine (*SI Appendix*, Fig. S26), while only stemmadenine was detected in incubations without acetyl CoA. The dataset highly enriched in *C. roseus* leaf epidermal transcripts contained a candidate acetyltransferase with 70% amino acid identity to vinorine synthase that was cloned and expressed in yeast together with GO, Redox1, and Redox2. When provided with 19*E*-geissoschizine this yeast strain accumulated an MIA (*m*/*z* 397) (*SI Appendix*, Fig. S21) shown by NMR analysis to be *O*-acetylstemmadenine (OAS) (*SI Appendix*, Figs. S27–S29 and Tables S1 and S2). Similarly, the recombinant acetyltransferase purified (*SI Appendix*, Fig. S31) from *E. coli* (Fig. 2*B* and *SI Appendix*, Fig. S30) and crude *C. roseus* leaf proteins (*SI Appendix*, Fig. S30) both converted stemmadenine to OAS in the presence of acetyl CoA. As a result, this enzyme was named stemmadenine-*O*-acetyltransferase (SAT). VIGS suppression of SAT by 78.7% did not diminish catharanthine or vindoline levels significantly, but low levels of stemmadenine (0.124 $mg{\cdot}g^{-1}$ fresh leaf) could be detected in silenced plants compared with EV controls where this MIA was not detectable (Fig. 1 *A* and *F* and *SI Appendix*, Fig. S1).

An Additional NADPH-Dependent Enzymatic Step Is Required to Complete the Catharanthine/Tabersonine Pathway. The role of OAS in the assembly of catharanthine/tabersonine was tested by incubating it with crude *C. roseus* leaf protein. Enzyme assays with boiled leaf protein extracts, OAS ± NADPH, did not convert OAS into other products (Fig. 2*C*). Enzyme assays with fresh protein extracts in the absence of NADPH catalyzed the disappearance of OAS (Fig. 2*C*), suggesting that under these conditions OAS was converted into a highly reactive intermediate that was not detected by LC- MS. Enzyme assays with *C. roseus* protein containing NADPH converted OAS to tabersonine (Fig. 2*C*, peak 15) and to trace levels of catharanthine (Fig. 2*C*, peak 1). Addition of recombinant HL2 to the assay eliminated the formation of catharanthine, but did not significantly increase the production of tabersonine (Fig. 2*C*), while addition of HL1 to the assay converted OAS to catharanthine (Fig. 2*C*, peak 1) at the expense of tabersonine (Fig. 2*C*, peak 15). These results clearly suggest that HL1 together with an NADPH requiring reaction found in *C. roseus* leaves are necessary for conversion of OAS to catharanthine. The ready conversion of OAS to tabersonine in the presence of NADPH suggested that crude extracts may have high native HL2 activity, making it difficult to show the role of HL2 suggested by VIGS experiments (Fig. 1) in the assembly of tabersonine.

To better address HL2 activity, crude leaf proteins of *Tabernamonana litoralis* was employed. *T. litoralis* produces aspidosperma MIAs such as tabersonine and iboga MIAs, such as coronaridine, but not catharanthine (21). Enzyme assays with *T. litoralis* protein containing NADPH converted OAS to tabersonine (Fig. 2*D*, peak 15), but no catharanthine formation was detected. Addition of recombinant HL2 to the assay increased the formation of tabersonine (Fig. 2*D*, peak 15) by 100%, while enzyme assays with HL1 resulted in the formation of catharanthine (Fig. 2*D*, peak 1) at the expense of tabersonine (Fig. 2*D*, peak 15) that declined by 80% compared with assays without either recombinant enzyme. These results (Fig. 2) together with VIGS studies (Fig. 1) show that OAS serves as a common intermediate used by an NADPH-requiring enzyme to form a hypothesized common reactive secodine-type intermediate (1) that is *O*-acetylated before it can be used as a substrate by HL1 to form catharanthine and HL2 to form tabersonine.

Discussion

The present study provides the basic framework for an eight-gene pathway (Fig. 3) required for the assembly of catharanthine and tabersonine from 4,21-dehydrogeissoschizine and describes several reactive pathway intermediates for elaboration of four major MIA skeletons belonging to the (*i*) corynanthean (geissoschizine and isositsirikine), (*ii*) strychnos (akuammicine, stemmadenine,

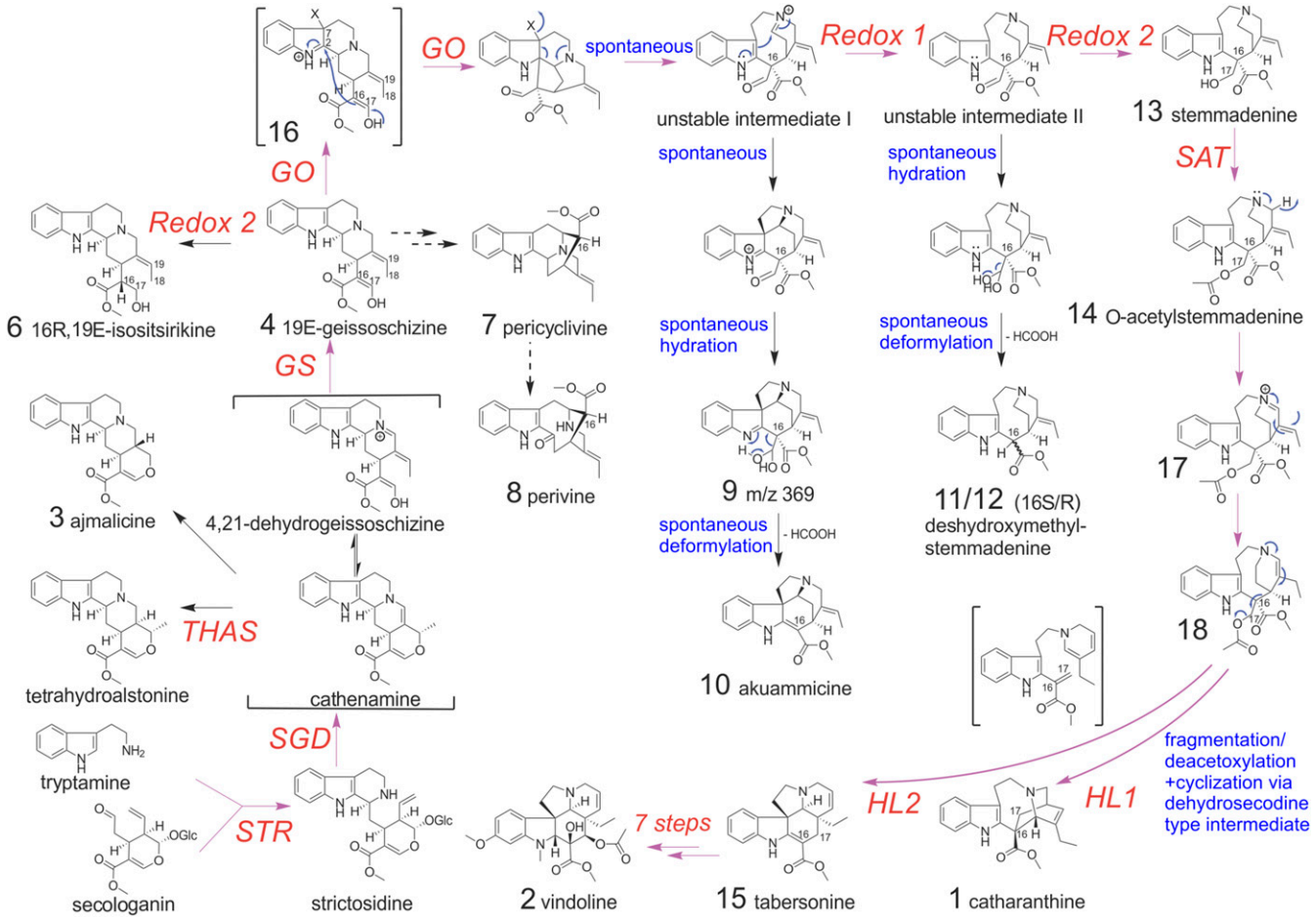

Fig. 3. The formation of catharanthine and tabersonine from 4,21 dehydrogeissoshizine involves GS, GO, Redox1, Redox2, SAT, an NADPH requiring reaction, HL1, and HL2. Pathway intermediates are involved in the elaboration of four major MIA skeletons: (*i*) corynanthean (geissoschizine and isositsirikine), (*ii*) strychnos (akuammicine, stemmadenine, OAS, and DHS), (*iii*) iboga (catharanthine), and (*iv*) aspidosperma (tabersonine). Pink arrows indicate the major biosynthetic route in *C. roseus*, and dashed arrows indicate hypothetical steps.

OAS, and DHS), (*iii*) iboga (catharanthine), and (*iv*) aspidosperma (tabersonine) classes of MIAs. The MIA intermediates provide a framework for the metabolic plasticity observed through the evolution of appropriate biochemical catalysts leading to the diversity of MIAs that have appeared in nature.

Concerted enzyme reactions involving GO, Redox1, and Redox2 are required for the formation of stemmadenine from 19*E*-geissoschizine (Fig. 2), since assays with GO alone led to the formation of akuammicine and a short-lived MIA (Fig. 2*A*) that was gradually converted to akuammicine (*SI Appendix*, Fig. S11) in VIGS–Redox1 plants (Fig. 1*A*), and assays with GO and Redox1 led to the formation of the epimeric DHS (Fig. 2*A*) also detected in VIGS–Redox2 plants (Fig. 1*A*). We speculate that GO catalyzes an oxidative rearrangement of 19*E*-geissoschizine involving oxidation of the latter compound to the 7-substituted indolenium **16,** which then undergoes an enol addition at C(2) followed by spontaneous fragmentation to restore aromaticity (Fig. 3). The resulting unstable intermediate I (Fig. 3) probably undergoes a spontaneous aldehyde hydration to form the short-lived MIA *m/z* 369, which was tentatively assigned the structure **9**, and thereafter deformylation to form akuammicine. Alternatively, intermediary indoleninium **16** could suffer a direct displacement at C(7) to give an akuammiline skeleton that would then rearrange to the same unstable intermediate I (22).

Iminium reduction of unstable intermediate I by Redox1 generates the unstable intermediate II (Fig. 3) that goes through spontaneous hydration and deformylation to give a mixture of epimeric 16*S*- and 16*R*-DHS. Finally, the aldehyde reduction on the unstable intermediate II by Redox2 forms stemmadenine, which stabilizes the molecule (Fig. 3). Although the exact mechanism could not be unambiguously determined in this study, it is worth noting that the Redox1-catalyzed iminium reduction on unstable intermediate I is likely analogous to the GS-catalyzed iminium reduction on 4,21-dehydrogeissoschizine (15), and both enzymes belong to the cinnamyl alcohol dehydrogenase family (54% amino acid identity). Similarly, Redox2-catalyzed aldehyde reduction on unstable intermediate II is analogous to the formation of isositsirikine from geissoschizine via the aldehyde intermediate (Fig. 3).

The formation of 19*E*-geissoschizine from 4,21-dehydrogeissoschizine by GS was suggested indirectly when strictosidine aglycone, composed of an equilibrium mixture of aglycones including 4,21-dehydrogeissoschizine, was converted to akuammicine when incubated in the presence of both GS and GO (16). The present study has used 19*E*-geissoschizine that could be generated directly from GS enzyme assays (15) to elaborate downstream steps in the catharanthine/tabersonine pathway. With the availability of 19*E*- and 19*Z*-geissoschizine we also show that Redox2 catalyzes an NADPH-stereospecific reduction to form 16*R*-isositsirikine that also accumulated in VIGS–GO plants (Fig. 1).

Biochemical acylation of functional groups may stabilize, protect, or activate the molecule for subsequent reactions in a biochemical pathway. The acetyl CoA-dependent biosynthesis of vinorine by vinorine synthase stabilizes the molecule for subsequent reactions in the biosynthesis of the antiarrhythmic drug ajmaline in *Rauvolfia serpentina* (23). In *Papaver somniferum* salutaridinol-7-*O*-acetyltransferase generates the activated benzylisoquinoline alkaloid, salutaridinol-7-*O*-acetate, leading to the spontaneous elimination of acetate to form thebaine (24), while acylation by 1,13-dihydroxy-*N*-methylcanadine-13-*O*-acetyltransferase protects the functional group from ring opening in the assembly of noscapine (25). Stemmadenine has been proposed as a key intermediate in the assembly of catharanthine and tabersonine based on chemistry (19) and feeding studies using *C. roseus* cell cultures (20). This study shows that stemmadenine only serves as a substrate after activation by SAT to form OAS that is converted through an uncharacterized NADPH-dependent enzyme reaction to form an unstable common *O*- acetylated secodine-type intermediate. The unstable nature of this intermediate might be the reason why OAS was lost when incubated with *C. roseus* leaf protein extracts without NADPH (Fig. 2).

Enzyme assays containing OAS and NADPH with *C. roseus* and/or *T. litoralis* leaf proteins showed that catharanthine was only formed (Fig. 2*C*) or its production is dramatically increased (Fig. 2*B*) by the addition of recombinant HL1. The high native HL2 activity in *C. roseus* leaf proteins prevented unambiguous assignment of HL2 function in vitro (Fig. 2*B*); however, tabersonine production was increased by 100% when recombinant HL2 was added to *T. litoralis* leaf proteins (Fig. 2*C*), providing strong biochemical evidence that HL2 is responsible for tabersonine formation. Together with clear results from VIGS studies (Fig. 1), we concluded that these two α/β hydrolase-type enzymes HL1 and HL2 (78% amino acid identity) specifically form catharanthine and tabersonine. We speculate OAS is oxidized and then suffers a 1,4-reduction by an NADPH-dependent enzyme of the conjugated iminium **17** (Fig. 3). The resulting enamine **18** is then deacetoxylated/fragmented, presumably in a synchronous process, to generate a dehydrosecodine-type intermediate by the action of HL1 and HL2, which also facilitate the following, at least formal, [4+2] cycloaddition to generate catharanthine and/or tabersonine, respectively (Fig. 3). The functions of the other two HL homologs, HL3 and HL4, were not studied in this report because of their low abundance in *C. roseus* leaves. Interestingly, only one HL homolog was found in the leaf total transcriptome of *V. minor* (https://bioinformatics.tugraz.at/phytometasyn/), a plant species known to accumulate aspidosperma, but not iboga type MIAs.

It is worth noting that the catharanthine/tabersonine pathway intermediates and breakdown products, such as 19*E*-geissoschizine, perivine, pericyclivine, 16*S*/*R*-DHS, and stemmadenine, are all secreted to the leaf surface. This is demonstrated by isolating these MIAs (Fig. 1*A* and *SI Appendix*, Fig. S1) using the leaf chloroform-dipping method developed for specific surface MIA extraction (13). Recently, MIAs of *V. minor* were shown to be secreted to the leaf surface too, and a *V. minor* vincamine exporter homologous to *C. roseus* catharanthine exporter CrTPT2 (14) was functionally characterized (26). These results corroborate suggestions (14) that MIA secretion may be a widespread phenomenon in MIA-producing plants.

We have now described and functionally characterized six genes as well as an additional NADPH-dependent seventh reaction required for the assembly of catharanthine/tabersonine from 19*E*-geissoschizine. These results together with the successful reconstitution in yeast of the strictosidine pathway (10) from geraniol and tryptophan and of the tabersonine to vindoline pathway (11) make it possible to reconstitute the multistep pathways for assembly of vindoline, catharanthine, and anticancer dimers, as well as several MIA skeletons in a heterologous host.

Materials and Methods

VIGS was conducted as described previously (5–8, 11) using primer sets described in *SI Appendix*, Table S3. Leaves were harvested 25–30 d after initiation of VIGS and processed for RNA isolation or for harvesting of leaf surface MIAs by chloroform dipping followed by methanol extraction to harvest MIAs within the leaf (12, 13). Leaves were directly extracted in ethyl acetate to obtain combined leaf surface and leaf body MIAs. MIAs were isolated from yeast using similar solvent systems and purified as described in *SI Appendix*.

ACKNOWLEDGMENTS. This work was supported by Natural Sciences and Engineering Research Council of Canada Discovery Grant (to V.D.L.), Canada Research Chairs (V.D.L.), and the Advanced Biomanufacturing Center (Brock University). Additional data reported in the study can be found in *SI Appendix*.

1. Szabó LF (2008) Rigorous biogenetic network for a group of indole alkaloids derived from strictosidine. *Molecules* 13:1875–1896.
2. De Luca V, Salim V, Atsumi SM, Yu F (2012) Mining the biodiversity of plants: a revolution in the making. *Science* 336:1658–1661.
3. Le Men L, Taylor WI (1965) A uniform numbering system for indole alkaloids. *Experientia* 21:508–510.
4. Tarselli MA, et al. (2011) Synthesis of conolidine, a potent non-opioid analgesic for tonic and persistent pain. *Nat Chem* 3:449–453.
5. Salim V, Wiens B, Masada-Atsumi S, Yu F, De Luca V (2014) 7-deoxyloganetic acid synthase catalyzes a key 3 step oxidation to form 7-deoxyloganetic acid in Catharanthus roseus iridoid biosynthesis. *Phytochemistry* 101:23–31.
6. Salim V, Yu F, Altarejos J, De Luca V (2013) Virus-induced gene silencing identifies *Catharanthus roseus* 7-deoxyloganic acid-7-hydroxylase, a step in iridoid and monoterpene indole alkaloid biosynthesis. *Plant J* 76:754–765.
7. Geu-Flores F, et al. (2012) An alternative route to cyclic terpenes by reductive cyclization in iridoid biosynthesis. *Nature* 492:138–142.
8. Asada K, et al. (2013) A 7-deoxyloganetic acid glucosyltransferase contributes a key step in secologanin biosynthesis in Madagascar periwinkle. *Plant Cell* 25:4123–4134.
9. Miettinen K, et al. (2014) The seco-iridoid pathway from *Catharanthus roseus*. *Nat Commun* 5:3606, and erratum (2014) 5:4175.
10. Brown S, Clastre M, Courdavault V, O'Connor SE (2015) De novo production of the plant-derived alkaloid strictosidine in yeast. *Proc Natl Acad Sci USA* 112:3205–3210.
11. Qu Y, et al. (2015) Completion of the seven-step pathway from tabersonine to the anticancer drug precursor vindoline and its assembly in yeast. *Proc Natl Acad Sci USA* 112:6224–6229.
12. Murata J, Roepke J, Gordon H, De Luca V (2008) The leaf epidermome of *Catharanthus roseus* reveals its biochemical specialization. *Plant Cell* 20:524–542.
13. Roepke J, et al. (2010) Vinca drug components accumulate exclusively in leaf exudates of Madagascar periwinkle. *Proc Natl Acad Sci USA* 107:15287–15292.
14. Yu F, De Luca V (2013) ATP-binding cassette transporter controls leaf surface secretion of anticancer drug components in *Catharanthus roseus*. *Proc Natl Acad Sci USA* 110:15830–15835.
15. Qu Y, et al. (2018) Geissoschizine synthase controls flux in the formation of monoterpenoid indole alkaloids in a *Catharanthus roseus* mutant. *Planta* 247:625–634.
16. Tatsis EC, et al. (2017) A three enzyme system to generate the Strychnos alkaloid scaffold from a central biosynthetic intermediate. *Nat Commun* 8:316.
17. Huang L, et al. (2012) Molecular characterization of the pentacyclic triterpenoid biosynthetic pathway in *Catharanthus roseus*. *Planta* 236:1571–1581.
18. Hirata T, Lee S-L, Scott AI (1979) Biosynthesis of (16R)-isositsirikine from geissoschizine with a cell-free extract of *Catharanthus roseus* callus. *J Chem Soc Chem Commun* 23:1081–1083.
19. Scott AI (1970) Biosynthesis of the indole alkaloids. *Acc Chem Res* 3:151–157.
20. El-Sayed M, Choi YH, Frédérich M, Roytrakul S, Verpoorte R (2004) Alkaloid accumulation in *Catharanthus roseus* cell suspension cultures fed with stemmadenine. *Biotechnol Lett* 26:793–798.
21. Qu Y, Simionescu R, De Luca V (2016) Monoterpene indole alkaloids from the fruit of *Tabernaemontana litoralis* and differential alkaloid composition in various fruit components. *J Nat Prod* 79:3143–3147.
22. Benayad S, Ahamada K, Lewin G, Evanno L, Poupon E (2016) Preakuammicine: A long-awaited missing link in the biosynthesis of monoterpene indole alkaloids. *Eur J Org Chem* 2016:1494–1499.
23. Bayer A, Ma X, Stöckigt J (2004) Acetyltransfer in natural product biosynthesis—functional cloning and molecular analysis of vinorine synthase. *Bioorg Med Chem* 12:2787–2795.
24. Grothe T, Lenz R, Kutchan TM (2001) Molecular characterization of the salutaridinol 7-*O*-acetyltransferase involved in morphine biosynthesis in opium poppy *Papaver somniferum*. *J Biol Chem* 276:30717–30723.
25. Dang TTT, Chen X, Facchini PJ (2015) Acetylation serves as a protective group in noscapine biosynthesis in opium poppy. *Nat Chem Biol* 11:104–106.
26. Demessie Z, Woolfson KN, Yu F, Qu Y, De Luca V (2017) The ATP binding cassette transporter, VmTPT2/VmABCG1, is involved in export of the monoterpenoid indole alkaloid, vincamine in *Vinca minor* leaves. *Phytochemistry* 140:118–124.